

1 **Identification of oxygen-independent pathways for pyridine-**
2 **nucleotide and Coenzyme-A synthesis in anaerobic fungi by**
3 **expression of candidate genes in yeast**

4

5 Thomas Perli[†], Aurin M. Vos[†], Jonna Bouwknecht, Wijnb J. C. Dekker, Sanne J. Wiersma,
6 Christiaan Mooiman, Raúl A. Ortiz-Merino, Jean-Marc Daran, Jack T. Pronk*

7 Department of Biotechnology, Delft University of Technology, Van der Maasweg 2629
8 Delft, The Netherlands.

9 *Corresponding author: Department of Biotechnology, Delft University of Technology,
10 Van der Maasweg 9, 2629 Delft, The Netherlands. Tel: +31-15-27-83214; E-mail:
11 J.T.Pronk@tudelft.nl

12 [†]These authors contributed equally.

13

14	Thomas Perli	T.Perli@tudelft.nl	0000-0002-4910-3292
15	Aurin M. Vos	A.M.Vos@tudelft.nl	
16	Jonna Bouwknecht	J.Bouwknecht@tudelft.nl	0000-0316-1238-7873
17	Wijnb J. C. Dekker	W.J.C.Dekker@tudelft.nl	
18	Sanne J. Wiersma	S.J.Wiersma@tudelft.nl	
19	Christiaan Mooiman	C.Mooiman@tudelft.nl	
20	Raúl A. Ortiz-Merino	Raul.Ortiz@tudelft.nl	0000-0003-4186-8941
21	Jean-Marc Daran	J.G.Daran@tudelft.nl	0000-0003-3136-8193
22	Jack T. Pronk	J.T.Pronk@tudelft.nl	0000-0002-5617-4611

23 **Abstract**

24 Neocallimastigomycetes are rare examples of strictly anaerobic eukaryotes. This study
25 investigates how these anaerobic fungi bypass reactions involved in synthesis of pyridine
26 nucleotide cofactors and coenzyme A that, in canonical fungal pathways, require
27 molecular oxygen. Analysis of Neocallimastigomycete proteomes identified a candidate L-
28 aspartate-decarboxylase (AdcA), and L-aspartate oxidase (NadB) and quinolinate
29 synthase (NadA), constituting putative oxygen-independent bypasses for coenzyme A
30 synthesis and pyridine nucleotide cofactor synthesis, respectively. The corresponding
31 gene sequences indicated acquisition by ancient horizontal gene transfer event involving
32 bacterial donors. To test whether these enzymes suffice to bypass corresponding oxygen-
33 requiring reactions, they were introduced into *fms1Δ* and *bna2Δ* *Sacharomyces cerevisiae*
34 strains. Expression of *nadA* and *nadB*, and *adcA* from the Neocallimastigomycetes
35 *Piromyces finnis* and *Neocallimastix californiae*, respectively, conferred cofactor
36 prototrophy under aerobic and anaerobic conditions. This study simulates how
37 horizontal gene transfer can drive eukaryotic adaptation to anaerobiosis, and provides a
38 basis for elimination of auxotrophic requirements in anaerobic industrial applications of
39 yeasts and fungi.

40

41 **Introduction**

42 Neocallimastigomycetes are obligately anaerobic fungi with specialised metabolic
43 adaptations that allow them to play a key role in the degradation of recalcitrant plant
44 biomass in herbivore guts [1]. Despite complicated cultivation techniques and lack of
45 genetic-modification tools [2], several evolutionary adaptations of these eukaryotes to an
46 anaerobic lifestyle have been inferred from biochemical studies [3-5]. Sequence analysis
47 implicated extensive horizontal gene transfer (HGT) events as a key mechanism in these
48 adaptations [6-8]. For example, instead of sterols, which occur in membranes of virtually
49 all other eukaryotes [9] and whose biosynthesis involve multiple oxygen-dependent
50 reactions [10], Neocallimastigomycetes contain tetrahymanol [3, 6]. This sterol surrogate
51 [11] can be formed from squalene by a squalene:tetrahymanol cyclase (STC), whose
52 structural gene in Neocallimastigomycetes showed evidence of acquisition by HGT from
53 prokaryotes [6, 12]. Expression of an STC gene was recently shown to enable sterol-
54 independent anaerobic growth of the model eukaryote *S. cerevisiae* [13].

55 Further exploration of oxygen-independent bypasses in Neocallimastigomycetes for
56 intracellular reactions that in other eukaryotes require oxygen is relevant for a
57 fundamental understanding of the requirements for anaerobic growth of eukaryotes. In
58 addition, it may contribute to the elimination of nutritional requirements in industrial
59 anaerobic applications of yeasts and fungi.

60 Most fungi are capable of *de novo* synthesis of pyridine-nucleotide cofactors (NAD⁺ and
61 NADP⁺) and Coenzyme A (CoA) when grown aerobically. As exemplified by the
62 facultatively anaerobic yeast *S. cerevisiae* [14], canonical fungal pathways for synthesis of
63 these cofactors are oxygen dependent. In *S. cerevisiae*, biosynthesis of CoA involves
64 formation of β -alanine by the oxygen-requiring polyamine oxidase Fms1 [15]. This
65 intermediate is then condensed with pantoate to yield the CoA precursor pantothenate

66 [16, 17] (Fig. 1A). Similarly, the yeast kynurenine pathway for *de novo* synthesis of NAD⁺
67 involves three oxygen-dependent reactions, catalyzed by indoleamine 2,3-dioxygenase
68 (Bna2; EC 1.13.11.52), kynurenine 3-monooxygenase (Bna4; EC 1.14.13.9), and 3-
69 hydroxyanthranilic-acid dioxygenase (Bna1; EC 1.13.11.6) [14] (Fig. 1B). The
70 Neocallimastigomycete *Neocallimastix patricianum* has been shown to grow in synthetic
71 media lacking precursors for pyridine-nucleotide and CoA synthesis [18]. This
72 observation indicates that at least some anaerobic fungi harbour oxygen-independent
73 pathways for synthesizing these essential cofactors. Genomes of Neocallimastigomycetes
74 lack clear homologs of genes encoding the oxygen-requiring enzymes of the kynurenine
75 pathway. Instead, their genomes were reported to harbour genes encoding an L-aspartate
76 oxidase (NadB) and quinolinate synthase (NadA), two enzymes active in the bacterial
77 pathway for NAD⁺ synthesis [6] (Fig. 1A). Since bacterial and plant aspartate oxidases can,
78 in addition to oxygen, also use fumarate as electron acceptor [19, 20], it is conceivable
79 that NadA and NadB may allow for oxygen-independent NAD⁺ synthesis in anaerobic
80 fungi. No hypothesis has yet been forwarded on how these fungi may bypass the oxygen
81 requirement for the canonical fungal CoA biosynthesis route.

82 The goals of this study were to identify the pathway responsible for oxygen-independent
83 synthesis of CoA in Neocallimastigomycetes and to investigate a possible role of NadA and
84 NadB in oxygen-independent synthesis of pyridine-nucleotide cofactors. A candidate L-
85 aspartate decarboxylase (Adc) encoding gene was identified by genome analysis of
86 Neocallimastigomycetes and its phylogeny investigated. Candidate
87 Neocallimastigomycete genes for L-aspartate oxidase and quinolinate synthase,
88 previously reported to have been acquired by HGT [6], as well as the candidate Adc gene,
89 were then functionally analysed by expression in *S. cerevisiae* strains devoid of essential
90 steps in the native cofactor synthesis pathways. As controls, previously characterized

91 genes involved in oxygen-independent NAD⁺ biosynthesis by *Arabidopsis thaliana* [21],
92 and a previously characterized Adc encoding gene from the red flour beetle *Tribolium*
93 *castaneum* (*TcPAND*) [22] were also expressed in the same *S. cerevisiae* strains. The
94 results demonstrate how heterologous expression studies in yeast can provide insight
95 into evolutionary adaptations to anaerobic growth and selective advantages conferred by
96 proposed HGT events in Neocallimastigomycetes. In addition, they identify metabolic
97 engineering strategies for eliminating oxygen requirements for cofactor biosynthesis in
98 anaerobic industrial applications of *S. cerevisiae*.

99 **Material and Methods**

100 **Strains, media and maintenance**

101 *S. cerevisiae* strains used and constructed in this study (Table 1) were derived from the
102 CEN.PK lineage [23]. Yeast cultures were routinely propagated in YP (10 g L⁻¹ Bacto yeast
103 extract [Becton, Dickinson and Co., Sparks, MD], 20 g L⁻¹ Bacto peptone [Becton, Dickinson
104 and Co]) or synthetic medium (SM) [24]. YP and SM were autoclaved at 121 °C for 20 min.
105 SM was then supplemented with 1 mL L⁻¹ of filter-sterilized vitamin solution (0.05 g L⁻¹
106 D-(+)-biotin, 1.0 g L⁻¹ D-calcium pantothenate, 1.0 g L⁻¹ nicotinic acid, 25 g L⁻¹ myo-inositol,
107 1.0 g L⁻¹ thiamine hydrochloride, 1.0 g L⁻¹ pyridoxol hydrochloride, 0.20 g L⁻¹ 4-
108 aminobenzoic acid). Where indicated, nicotinic acid or pantothenic acid were omitted
109 from the vitamin solution, yielding SM without nicotinic acid (SM Δ nic) and SM without
110 pantothenic acid (SM Δ pan), respectively. A concentrated glucose solution was autoclaved
111 separately for 15 min at 110 °C and added to SM and YP to a concentration of 20 g L⁻¹ or
112 50 g L⁻¹, yielding SMD and YPD, respectively. SMD with urea or acetamide instead of
113 ammonium sulfate (SMD-urea and SMD-Ac, respectively) were prepared as described
114 previously [25, 26]. For anaerobic growth experiments, sterile media were supplemented

115 with Tween 80 (polyethylene glycol sorbate monooleate, Merck, Darmstadt, Germany)
116 and ergosterol (≥ 95 % pure, Sigma-Aldrich, St. Louis, MO) as described previously [27].
117 Yeast strains were grown in 500-mL shake flasks containing 100 mL medium or in 100-
118 mL shake flasks containing 20 mL medium. Shake-flask cultures were incubated at 30 °C
119 and shaken at 200 rpm in an Innova Incubator (Brunswick Scientific, Edison, NJ). Solid
120 media were prepared by adding 15 g L⁻¹ Bacto Agar (Becton, Dickinson and Co) and, when
121 indicated, 200 mg L⁻¹ G418 (Thermo Scientific, Waltham, MA). After genotyping,
122 engineered strains were restreaked twice to select single clones. Removal of the gRNA
123 carrying plasmid was done as previously described [28]. Stock cultures were prepared by
124 adding glycerol to a final concentration of 33 % (v/v), frozen and stored at -80°C.

125 **Molecular biology techniques**

126 DNA was PCR amplified with Phusion Hot Start II High Fidelity Polymerase (Thermo
127 Scientific) and desalted or PAGE-purified oligonucleotide primers (Sigma Aldrich) by
128 following manufacturers' instructions. DreamTaq polymerase (Thermo Scientific) was
129 used for diagnostic PCR. Oligonucleotide primers used in this study are listed in
130 Supplementary Table S1. PCR products were separated by gel electrophoresis using 1 %
131 (w/v) agarose gel (Thermo Scientific) in TAE buffer (Thermo Scientific) at 100 V for 25
132 min and purified with either GenElute PCR Clean-Up Kit (Sigma Aldrich) or with
133 Zymoclean Gel DNA Recovery Kit (Zymo Research, Irvine, CA). Plasmids were purified
134 from *E. coli* using a Sigma GenElute Plasmid Kit (Sigma Aldrich). Yeast genomic DNA was
135 isolated with the SDS/LiAc protocol [29]. Yeast strains were transformed with the lithium
136 acetate method [30]. Four to eight single colonies were re-streaked three consecutive
137 times on selective media and diagnostic PCR were performed to verify their genotype.
138 *Escherichia coli* XL1-blue was used for chemical transformation [31]. Plasmids were then

139 isolated and verified by either restriction analysis or by diagnostic PCR. Lysogeny Broth
140 (LB; 10 g L⁻¹ Bacto Tryptone, 5 g L⁻¹, Bacto Yeast Extract with 5 g L⁻¹ NaCl) was used to
141 propagate *E. coli* XL1-Blue. LB medium was supplemented with 100 mg L⁻¹ ampicillin for
142 selection of transformants. The overnight grown bacterial cultures were stocked by
143 adding sterile glycerol at a final concentration of 33 % (v/v) after which samples were
144 frozen and stored at -80 °C.

145 **Plasmid construction**

146 Plasmids used and cloned in this study are shown in Table 2. Plasmids carrying two copies
147 of the same gRNA were cloned by Gibson assembly [28, 32]. In brief, an oligo carrying the
148 gene-specific 20 bp target sequence and a homology flank to the plasmid backbone was
149 used to amplify the fragment carrying the 2µm origin of replication sequence by using
150 pROS13 as template. The backbone linear fragment was amplified using primer 6005 and
151 pROS11 as template [33]. The two fragments were then gel purified and assembled *in*
152 *vitro* using the NEBuilder HiFi DNA Assembly Master Mix (New England BioLabs, Ipswich,
153 MA) following manufacturer's instructions. Transformants were selected on LB plates
154 supplemented with 100 mg L⁻¹ ampicillin or 50 mg L⁻¹ kanamycin. Primer 11861 was used
155 to amplify the 2µm fragment containing two identical gRNA sequences for targeting *BNA2*.
156 The PCR product was then cloned in a pROS11 backbone yielding plasmid pUDR315.
157 The coding sequences for *AtNADA*, *AtNADB*, *Pfnada*, *Pfnadb*, and *Ncadca* were codon-
158 optimized for expression in *S. cerevisiae* and ordered as synthetic DNA through GeneArt
159 (Thermo Fisher Scientific). The plasmids carrying the expression cassettes for *TcPAND*,
160 *AtNADA*, *AtNADB*, *Pfnada* and *Pfnadb* were cloned by Golden Gate assembly using the
161 Yeast Toolkit (YTK) DNA parts [34]. These plasmids were cloned using the pYTK096
162 integrative backbone that carries long homology arms to the *URA3 locus* and a *URA3*

163 expression cassette allowing for selection on SM lacking uracil. The *TcPAND* coding
164 sequence was amplified using the primer pair 11877/11878 and pCfB-361 as template.
165 Then, the linear *TcPAND* gene and plasmids pUD1096, pUD1097, pUD652, and pUD653
166 carrying the coding sequence for *AtNADA*, *AtNADB*, *PfnadA*, and *PfnadB*, respectively, were
167 combined together with YTK-compatible part plasmids in BsaI (New England BioLabs)
168 golden gate reactions to yield plasmid pUDI168, pUDI245, pUDE931, pUDI243, and
169 pUDI244, respectively. A detailed list of the YTK-compatible parts used for constructing
170 each plasmid can be found in Supplementary Table S2.

171 The plasmid carrying the expression cassette for *Ncadca* was cloned by Gibson assembly.
172 The *pTDH3* promoter, the *Ncadca* coding sequence, the *tENO2* terminator and the
173 pYTK0096 backbone were amplified by PCR using primer pairs 16721/16722,
174 16723/16724, 16725/16726, and 16727/16728 respectively, using pYTK009, pUD1095,
175 pYTK055, and pYTK096 as template, respectively. Each PCR product was then gel purified
176 and combined in equimolar amounts in a Gibson reaction that yielded pUDI242.

177 **Strain construction**

178 *S. cerevisiae* strains were transformed using the LiAc/SS-DNA/PEG and CRISPR/Cas9
179 method [28, 30, 35]. For deletion of the *BNA2* gene, IMX585 (*can1Δ::Spycas9-natNT2*) was
180 transformed with 500 ng of the *BNA2* targeting gRNA plasmid pUDR315 together with
181 500 ng of the annealed primer pair 11862/11863 as repair dsDNA oligo, yielding strain
182 IMK877. The resulting strain was then used for the integration of the two heterologous
183 *NADB-A* pathways. Expression cassettes for *AtNADA*, *AtNADB*, *PfnadA*, *PfnadB*, were
184 amplified from plasmids pUDI245, pUDE931, pUDI243, pUDI244, respectively, using
185 primer pairs 13123/13124, 13125/10710, 13123/13124, 13125/10710, respectively.
186 Then, 500 ng of each pair of gel purified repair cassettes were co-transformed in IMK877

187 together with 500 ng the *SGA1* targeting gRNA plasmid, yielding IMX2302 (*sga1::AtNADA*
188 *AtNADB*) and IMX2301 (*sga1::PfnadA PfnadB*).

189 For deletion of the *FMS1* gene, IMX581 (*can1Δ::Spycas9-natNT2 ura3-52*) was
190 transformed with 500 ng of the *FMS1* targeting gRNA plasmid pUDR652 together with
191 500 ng of the annealed primer pair 13527/13528 as repair dsDNA oligo, resulting in
192 IMX2293. Then, 500 ng of plasmids pUDI168 and pUDI242 carrying the expression
193 cassettes for *TcPAND* and *NcadcA*, respectively, were NotI (Thermo Fisher) digested and
194 separately transformed in IMX2293, yielding IMX2305, and IMX2300, respectively.
195 Selection of IMX2305 and IMX2300 was done on SMD agar plate since the integration of
196 each Adc encoding cassette also restored the *URA3* phenotype. In contrast, selection of
197 IMK877 was done on SMD-Ac agar plates while selection of IMX2302, IMX2301, and
198 IMX2293 was done YPD-G418 agar plates. Strains IMK877, IMX2300, IMX2302, and
199 IMX2301 were stocked in SMD, while IMX2305 and IMX2293 were stocked in SMD Δ pan
200 and YPD, respectively.

201 **Aerobic growth studies in shake flasks**

202 For the determination of the specific growth rate of the engineered strains under aerobic
203 conditions, a frozen aliquot was thawed and used to inoculate a 20 mL wake-up culture
204 that was then used to inoculate a pre-culture in a 100 mL flask. The exponentially growing
205 pre-culture was then used to inoculate a third flask to an initial OD₆₆₀ of 0.2. The flasks
206 were then incubated, and growth was monitored using a 7200 Jenway Spectrometer
207 (Jenway, Stone, United Kingdom). Specific growth rates were calculated from at least five
208 time-points in the exponential growth phase of each culture. Wake-up and pre-cultures of
209 IMX2301 and IMX2302 were grown in SMD Δ nic. Wake-up and pre-cultures of IMX2300

210 and IMX2305 were grown in SMD Δ pan while wake-up and pre-cultures of IMK877 and
211 IMX2292 were grown in SMD.

212 **Anaerobic growth studies in shake flasks**

213 Anaerobic shake-flask based experiments were performed in Lab Bactron 300 anaerobic
214 workstation (Sheldon Manufacturing Inc., Cornelius, OR) containing an atmosphere of 85
215 % N₂, 10 % CO₂, and 5 % H₂. Flat-bottom shake flasks of 50-mL were filled with 40 mL
216 SMD-urea media containing 50 g L⁻¹ glucose as carbon source, to ensure depletion of the
217 vitamin/growth factor of interest, and 20 g L⁻¹ glucose for the first transfer. Media were
218 supplemented with vitamins, with and without pantothenic acid or nicotinic acid as
219 indicated, and in all cases supplemented with Tween 80 and ergosterol. Sterile medium
220 was placed inside the anaerobic chamber 24 h prior to inoculation for removal of oxygen.
221 Traces of oxygen were continuously removed with a regularly regenerated Pd catalyst for
222 H₂-dependent oxygen removal placed inside the anaerobic chamber. Aerobic overnight
223 shake-flask cultures on SMD-urea were used to inoculate the anaerobic shake flask
224 without pantothenic acid or without nicotinic acid at an initial OD₆₀₀ of 0.2. Cultures were
225 cultivated at 30 °C with continuous stirring at 240 rpm on IKA KS 260 Basic orbital shaker
226 platform (Dijkstra Verenigde BV, Lelystad, the Netherlands). Periodic optical density
227 measurements at a wavelength of 600 nm using an Ultrospec 10 cell density meter
228 (Biochrom, Cambridge, United Kingdom) inside the anaerobic environment were used to
229 follow the growth over time. After growth had ceased and the OD₆₀₀ no longer increased
230 the cultures were transferred to SMD-urea with 20 g L⁻¹ glucose at an OD₆₀₀ of 0.2 [27].

231 **Anaerobic bioreactor cultivation**

232 Anaerobic bioreactor batch cultivation was performed in 2-L laboratory bioreactors
233 (Applikon, Schiedam, the Netherlands) with a working volume of 1.2 L. Bioreactors were

234 tested for gas leakage by applying 0.3 bar overpressure while completely submerging
235 them in water before autoclaving. Anaerobic conditions were maintained by continuous
236 sparging of the bioreactor cultures with 500 mL N₂ min⁻¹ (≤ 0.5 ppm O₂, HiQ Nitrogen 6.0,
237 Linde Gas Benelux, Schiedam, the Netherlands). Oxygen diffusion was minimized by using
238 Fluran tubing (14 Barrer O₂, F-5500-A, Saint-Gobain, Courbevoie, France) and Viton O-
239 rings (Eriks, Alkmaar, the Netherlands). Bioreactor cultures were grown on either
240 SMD Δ pan or SMD Δ nic with ammonium sulfate as nitrogen source. pH was controlled at 5
241 using 2 M KOH. The autoclaved mineral salts solution was supplemented with 0.2 g L⁻¹
242 sterile antifoam emulsion C (Sigma-Aldrich). Bioreactors were continuously stirred at 800
243 rpm and temperature was controlled at 30 °C. Evaporation of water and volatile
244 metabolites was minimized by cooling the outlet gas of bioreactors to 4 °C in a condenser.
245 The outlet gas was then dried with a PermaPure PD-50T-12MPP dryer (Permapure,
246 Lakewood, NJ) prior to analysis. CO₂ concentrations in the outlet gas were measured with
247 an NGA 2000 Rosemount gas analyser (Emerson, St. Louis, MO). The gas analyser was
248 calibrated with reference gas containing 3.03 % CO₂ and N6-grade N₂ (Linde Gas Benelux,
249 Schiedam, The Netherlands).

250 Frozen glycerol stock cultures were used to inoculate aerobic 100 mL shake flask cultures
251 on either SMD Δ pan or SMD Δ nic. Once the cultures reached OD₆₆₀ > 5, a second 100 mL
252 aerobic shake-flask pre-culture on the same medium was inoculated. When this second
253 pre-culture reached the exponential growth phase, biomass was harvested by
254 centrifugation at 3000 g for 5 min and washed with sterile demineralized water. The
255 resulting cell suspension was used to inoculate anaerobic bioreactors at an OD₆₆₀ of 0.2.

256 **Analytical methods**

257 Biomass dry weight measurements of the bioreactor batch experiments were performed
258 using pre-weighed nitrocellulose filters (0.45 μm , Gelman Laboratory, Ann Arbor, MI). 10
259 mL culture samples were filtrated and then the filters were washed with demineralized
260 water prior to drying in a microwave oven (20 min at 360 W) and weight measurement.
261 Metabolite concentrations in culture supernatants were analysed by high-performance
262 liquid chromatography (HPLC). In brief, culture supernatants were loaded on an Agilent
263 1260 HPLC (Agilent Technologies, Santa Clara, CA) fitted with a Bio-Rad HPX 87 H column
264 (Bio-Rad, Hercules, CA). The flow rate was set at 0.6 mL min⁻¹ and 0.5 g L⁻¹ H₂SO₄ was used
265 as eluent. An Agilent refractive-index detector and an Agilent 1260 VWD detector were
266 used to detect culture metabolites [36]. An evaporation constant of 0.008 divided by the
267 volume in liters, was used to correct HPLC measurements of ethanol in the culture
268 supernatants, taking into account changes in volume caused by sampling [37]. Statistical
269 analysis on product yields was performed by means of an unpaired two-tailed Welch's t-
270 test.

271 **Homology and phylogenetic analyses**

272 A set of 51 aminoacid sequences previously used to discriminate between glutamate
273 decarboxylases and L-aspartate decarboxylases [38] was re-used to identify candidate
274 Neocallimastigomycete Adc sequences. These sequences were used as queries against a
275 database containing all 58109 Neocallimastigomycete proteins deposited in Uniprot
276 trembl (Release 2019_02), which represented 5 species (*Neocallimastix californiae*,
277 *Anaeromyces robustus*, *Piromyces sp E2*, *Piromyces finnis*, and *Pecoramyces ruminatum*),
278 and extracted according to the NCBI taxid 451455. Sequence homology was analysed
279 using BLASTP 2.6.0+ [39] with 10⁻⁶ as e-value cut-off resulting in 13

280 Neocallimastigomycete sequences as shared hits from all 51 queries (Supplementary
281 Table S3). Four of these sequences showing homology to experimentally characterised
282 proteins with L-aspartate-decarboxylase (Adc) activity originated from *N. californiae*, and
283 were checked for RNAseq read coverage and splicing junction support revealing
284 A0A1Y1ZL74 as best candidate (Supplementary Fig. S1).

285 A0A1Y1ZL74, also referred to as *NcadcA*, was used for a second round of homology search
286 using HMMER 3.2 [40] against a database with a balanced representation of taxa across
287 the 3 domains of life. This database was built from Uniprot Release 2019_02 to include all
288 refseq sequences from Bacteria (taxid 2), Eukarya (taxid 2759), and Archaea (taxid 2157;
289 TrEMBL and Swiss-Prot categories were also included in this case). Selection for hits with
290 more than 60% alignment length and evalue $< 10^{-6}$ resulted in a total of 325 sequences
291 (103 from Bacteria, 101 from Eukaryotes, and 121 from Archaea).

292 The set of 325 A0A1Y1ZL74 homologous sequences, together with those from Tomita *et*.
293 *al.* (2015) [38] were aligned with Clustal Omega 1.2.4 [41] and then used to build a
294 maximum likelihood phylogenetic tree with RAxML-NG 0.8.1 [42] using default
295 parameters with the exception of the use of the PROTGTR+FO model and 100 bootstrap
296 replicates. The resulting phylogenetic tree drawn with iTOL [43] is shown in Fig. 2,
297 corresponding alignments and trees are provided in Supplementary Files 1 and 2.

298 Multiple sequence alignment was also performed with Clustal omega 1.2.4 [41] to
299 compare selected aminoacid sequences showing candidate and experimentally
300 characterised Adcs, against bacterial PanDs. These sequences and alignments are shown
301 in Supplementary File 3.

302 **Whole-genome sequencing and analysis.**

303 Genomic DNA of strains IMX2300 and IMX2300-1 was isolated with a Blood & Cell Culture
304 DNA Kit with 100/G Genomics-tips (QIAGEN, Hilden, Germany) according to the
305 manufacturers' instructions. The Miseq Reagent Kit v3 (Illumina, San Diego, CA), was used
306 to obtain 300 bp reads for paired-end sequencing. Genomic DNA was sheared to an
307 average of 550 bp fragments using an M220 ultrasonicator (Covaris, Wolburn, MA).
308 Libraries were prepared by using a TruSeq DNA PCR-Free Library Preparation kit
309 (Illumina) following manufacturer's instructions. The samples were quantified by qPCR
310 on a Rotor-Gene Q PCR cycler (QIAGEN) using the Collibri Library quantification kit
311 (Invitrogen Carlsbad, CA). Finally, the library was sequenced using an Illumina MiSeq
312 sequencer (Illumina, San Diego, CA) resulting in a minimum 50-fold read coverage.
313 Sequenced reads were mapped using BWA 0.7.15-r1142-dirty [44] against the
314 CEN.PK113-7D genome [45] containing an extra contig with the relevant integration
315 cassette. Alignments were processed using SAMtools 1.3.1 [46], and sequence variants
316 were called using Pilon 1.18 [47], processed with ReduceVCF 12
317 ([https://github.com/AbeelLab/genometools/blob/master/scala/abeel/genometools/re](https://github.com/AbeelLab/genometools/blob/master/scala/abeel/genometools/reducevcf/ReduceVCF.scala)
318 [ducevcf/ReduceVCF.scala](https://github.com/AbeelLab/genometools/blob/master/scala/abeel/genometools/reducevcf/ReduceVCF.scala)), and annotated using VCFannotator
319 (<http://vcfannotator.sourceforge.net/>) against GenBank accession GCA_002571405.2
320 [48].

321 **Data availability**

322 DNA sequencing data of the *Saccharomyces cerevisiae* strains IMX2300 and IMX2300-1
323 were deposited at NCBI (<https://www.ncbi.nlm.nih.gov/>) under BioProject accession
324 number PRJNA634013. All measurement data and calculations used to prepare Fig. 3-4
325 and Tables 3-4 of the manuscript are available at the 4TU.Centre for research data

326 repository (<https://researchdata.4tu.nl/>) under doi: 10.4121/uuid:c3d2326d-9ddb-
327 469a-b889-d05a09be7d97.

328 **Results**

329 **Identification of a candidate oxygen-independent L-aspartate decarboxylase** 330 **involved in CoA synthesis in anaerobic fungi**

331 Decarboxylation of L-aspartate to β -alanine by L-aspartate decarboxylase (Adc), an
332 enzyme that occurs in all domains of life [38], enables an oxygen-independent alternative
333 for the canonical fungal pathway for CoA synthesis (Fig. 1A). A set of 51 amino acid
334 sequences of Adcs homologs listed by Tomita *et al.* (2015)[38] were used as queries
335 against all Neocallimastigomycete proteins deposited in the TrEMBL section of the
336 UNIPROT database. This search yielded 13 Neocallimastigomycete hits (e-value < 10^{-6} ,
337 Supplementary Table S3), 4 of which originated from *N. californiae*. Only one of these hits,
338 A0A1Y1ZL74, did not reveal annotation errors upon RNAseq read mapping and showed
339 the highest read coverage (Supplementary Fig. S1) and was selected as best candidate Adc
340 encoding gene.

341 The sequence A0A1Y1ZL74 (hereafter referred to as *NcAdcA*) was used for a second round
342 of homology search against a broader set of Adc sequences, with a similar sequence
343 representation of taxa across the 3 domains of life (103 sequences from Bacteria, 101
344 from Eukarya, and 121 from Archaea). The resulting set of *NcAdcA* homologs, together
345 with the set defined by Tomita *et al.* (2015) [38], were subjected to multiple sequence
346 alignment. A subsequent phylogenetic tree (Fig. 2) showed that *NcAdc* sequences are
347 closely related to those of chytrid fungi (A0A0L0HIP1 from *Spizellomyces punctatus*,
348 A0A1S8W5A4 from *Batrachochytrium salamandrivorans* and F4NWP2 from
349 *Batrachochytrium dendrobatidis*) and from the rumen-associated anaerobic bacterium

350 *Clostridium cellulolyticum* (B8I983). Neocallimastigomycete, chytrid and *C. cellulolyticum*
351 Adc homologs were more closely related to each other than to characterised eukaryotic
352 Adc and bacterial PanD sequences. These results indicate that an ancestor of *C.*
353 *cellulolyticum* donated an Adc-encoding sequence to a common ancestor of chytrids and
354 Neocallimastigomycetes.

355 Comparison of bacterial PanDs (Q0TLK2 from *E. coli* and P9WIL2 from *Mycobacterium*
356 *tuberculosis*) against Adcs from other bacteria (B8I983 from *C. cellulolyticum*), and
357 eukaryotes (including A7U8C7 from *Tribolium castaneum*) showed only little sequence
358 homology between *NcAdcs*, known bacterial PanDs, and eukaryotic Adcs (Supplementary
359 File 3). The only conserved region encompassed the full length of PanDs (126-139 amino
360 acids), which represents less than 60 % of the full length of other Adc sequences (*e.g.*
361 *NcAdcA* is 625 amino acids long).

362 **Neocallimastigomycete *PfnadB*, *PfnadA* and *NcadCA* genes support aerobic** 363 **pyridine-nucleotide and CoA synthesis in yeast.**

364 Neocallimastigomycetes were previously reported to have acquired an L-aspartate
365 oxidase (*nadB*) and a quinolinate synthase gene (*nadA*) by HGT [6]. Hence, UNIPROT
366 entries A0A1Y1V2P1 and A0A1Y1VAT1 from *Piromyces finnis* were functionally
367 reassigned as NadA and NadB candidates and the corresponding genes were tentatively
368 named *PfnadB* and *PfnadA*. These sequences, together with *NcadCA*, were codon-
369 optimised and tested to bypass the corresponding oxygen-requiring reactions in *S.*
370 *cerevisiae*.

371 The *BNA2* and *FMS1* genes of *S. cerevisiae* were deleted by Cas9-mediated genome editing.
372 The inability of strain IMK877 (*bnaz2Δ*) to synthesize quinolinic acid and of strain
373 IMX2292 (*fms1Δ*) to synthesize β -alanine was evident from their inability to grow on

374 glucose synthetic medium (SMD) lacking nicotinic acid or pantothenate, respectively
375 (Table 3). Strain IMK877 was used for heterologous complementation studies with
376 codon-optimized expression cassettes for *PfnadB* and *PfnadA*, while an expression
377 cassette for *N. californiae NcadcA* (A0A1Y1ZL74) was introduced into strain IMX2292.
378 Congenic strains expressing previously characterized *NADB* and *NADA* genes from
379 *Arabidopsis thaliana* (*AtNadB* and *AtNadA*, Q94AY1 and Q9FGS4)[21], and a previously
380 characterized gene from *Tribolium castaneum* encoding an aspartate decarboxylase
381 (*TcPanD*, A7U8C7)[22] were tested in parallel.

382 Aerobic growth of the engineered *S. cerevisiae* strains was characterized in shake-flask
383 cultures on SMD or on either SMD Δ nic or SMD Δ pan (Table 1). In contrast to the reference
384 strain IMK877 (*bnad2*), *S. cerevisiae* IMX2301 (*bnad2 PfnadB PfnadA*) grew in SMD Δ nic,
385 indicating complementation of the *bnad2*-induced nicotinate auxotrophy by *PfnadB* and
386 *PfnadA*. However, the specific growth rate of the engineered strain in these aerobic
387 cultures was approximately 3-fold lower than that of the reference strain IMX585 (*BNA2*,
388 Table 1). Strain IMX2302 (*bnad2 AtNADB AtNADA*) did not grow in SMD Δ nic, suggesting
389 that the plant *NadB* and/or *NadA* proteins were either not functionally expressed or not
390 able to complement the nicotinate auxotrophy in these aerobic yeast cultures.

391 Strain IMX2300 (*fms1 Δ NcadcA*) grew in SMD Δ pan, indicating complementation of the
392 pantothenate auxotrophy. However, this strain reproducibly showed a lag phase of
393 approximately 48 h upon its first transfer from SMD to SMD Δ pan, and grew exponentially
394 thereafter at a rate of $0.34 \pm 0.01 \text{ h}^{-1}$. To explore whether the lag phase of strain IMX2300
395 reflected selection of a spontaneous mutant, it was subjected to three sequential transfers
396 in SMD Δ pan. A single-colony isolate, IMX2300-1 from the adapted population showed a
397 specific growth rate of $0.34 \pm 0.01 \text{ h}^{-1}$ in both SMD and SMD Δ pan (Table 1). Whole-genome
398 sequencing of IMX2300-1 did not reveal any mutations in coding DNA sequences that

399 were considered physiologically relevant in this context when compared to the non-
400 adapted strain IMX2300 (Bioproject accession number: PRJNA634013). When both
401 strains were compared to the reference CEN.PK113-7D sequence [45], a total of 16
402 mutations were found including eight non-synonymous and eight synonymous, with
403 most mutations occurring in either Y' helicases or Ty elements (Supplementary File 4).
404 These elements resided in highly repetitive chromosomal regions and were therefore
405 prone to biased variant calling when using short-read sequencing technologies. The only
406 non-synonymous mutation found in both IMX2300 and IMX2300-1 involved a leucine to
407 methionine change in amino acid 315 of an Mtm1 homolog predicted to be a high affinity
408 pyridoxal 5'-phosphate (PLP) transporter, involved in delivery of the PLP cofactor to
409 mitochondrial enzymes. Overall, these observations indicate that the lag phase of strain
410 IMX2300 most likely reflected a physiological adaptation or culture heterogeneity rather
411 than a mutational event [49].

412 The specific growth rate of *S. cerevisiae* IMX2305 (*fms1Δ TcPAND*) on SMD Δ pan did not
413 significantly differ from that of the reference strain IMX585 on SMD, and it was almost
414 four-fold higher than the specific growth rate of the reference strain on SMD Δ pan. These
415 results are consistent with a previous study on functional expression of *TcPAND* in *S.*
416 *cerevisiae* [50].

417 **Expression of Neocallimastigomycete *PfnadB*, *PfnadA*, and *NcadcA* suffice to** 418 **enable anaerobic pyridine-nucleotide and CoA synthesis in yeast**

419 To investigate whether expression of heterologous *PfnadB*, *PfnadA*, and *NcadcA* was
420 sufficient to enable anaerobic growth in the absence of nicotinate and pantothenate,
421 respectively, growth of the engineered *S. cerevisiae* strains on SMD, SMD Δ nic and/or
422 SMD Δ pan was monitored in an anaerobic chamber (Fig. 3).

423 Growth experiments on SMD Δ nic or SMD Δ pan were preceded by a cultivation cycle on the
424 same medium, supplemented with 50 g L⁻¹ instead of 20 g L⁻¹ of glucose to ensure
425 complete depletion of any surplus cellular contents of pyridine nucleotides, CoA, or
426 relevant intermediates. Indeed, upon a subsequent transfer to SMD Δ nic or SMD Δ pan, the
427 reference strain IMX585 (*BNA2 FMS1*), expressing the native oxygen-dependent
428 pathways for nicotinate and β -alanine synthesis, showed no growth (Fig. 3 panels A, B and
429 C).

430 Both engineered strains IMX2301 (*bnaz2 Δ PfnadB PfnadA*) and IMX2302 (*bnaz2 Δ AtNADB*
431 *AtNADA*) grew anaerobically on SMD Δ nic. This provided a marked contrast with the
432 aerobic growth studies on this medium, in which strain IMX2302 did not grow. Strains
433 IMX2305 (*fms1 Δ TcPAND*) and the aerobically pre-adapted IMX2300-1 (*fms1 Δ NcadcA*)
434 both grew on SMD Δ pan under anaerobic conditions (Fig. 3 panels D, E and F).

435 **Characterization of engineered yeast strains in anaerobic batch bioreactors**

436 The anaerobic chamber experiments did not allow quantitative analysis of growth and
437 product formation. Therefore, growth of the *S. cerevisiae* strains expressing the
438 Neocallimastigomycetes genes, IMX2301 (*bnaz2 Δ PfnadB PfnadA*) and IMX2300-1 (*fms1 Δ*
439 *NcadcA*) was studied in anaerobic bioreactor batch cultures on SMD Δ nic or SMD Δ pan and
440 compared with growth of *S. cerevisiae* IMX585 (*BNA2 FMS1*) on the same media.

441 The reference strain IMX585, which typically grows fast and exponentially in anaerobic
442 bioreactors when using complete SMD [51], exhibited extremely slow, linear growth on
443 SMD Δ nic and SMD Δ pan (Fig. 4). Similar growth kinetics in ‘anaerobic’ bioreactor cultures
444 of *S. cerevisiae* on synthetic medium lacking the anaerobic growth factors Tween 80 and
445 ergosterol were previously attributed to slow leakage of oxygen into laboratory
446 bioreactors [27, 52, 53].

447 In contrast to the reference strain IMX585, the engineered strains IMX2301 and IMX2300-
448 1 exhibited exponential anaerobic growth on SMD Δ nic and SMD Δ pan, respectively (Fig.
449 4; Table 2). The specific growth rate of strain IMX2301 (*bnad2 Δ PfnadB PfnadA*) on
450 SMD Δ nic was not significantly different from that of the reference strain on complete SMD
451 [51], indicating full complementation of the anaerobic nicotinate auxotrophy of *S.*
452 *cerevisiae*. The specific growth rate of strain IMX2300-1 (*fms1 Δ NcadcA*) on SMD Δ pan was
453 only 20 % lower than this benchmark (Table 2). Biomass and ethanol yields of strain
454 IMX2301 grown in anaerobic batch cultures on SMD Δ nic and strain IMX2300-1 grown on
455 SMD Δ pan were not significantly different from those of the reference strain IMX585
456 grown on complete SMD (p -value > 0.05, Table 2).

457 **Discussion**

458 This study shows how expression of *PfnadB*, *PfnadA*, and *NcadcA* genes from
459 Neocallimastigomycetes, as well as corresponding orthologs from other species (*AtNADB*,
460 *AtNADA*, and *TcPAND*), confer oxygen-independent nicotinate and panthotenate
461 prototrophy to the facultatively anaerobic yeast *S. cerevisiae*. These results also provide
462 insights into how acquisition of these genes by HGT conferred selective advantage to
463 Neocallimastigomycete ancestors under anaerobic conditions.

464 Genomic analyses previously suggested that genomes of Neocallimastigomycetes encode
465 a putative L-aspartate oxidase (NadB) and quinolinate synthase (NadA) as alternatives to
466 the canonical kynurenine pathway found in other fungi [6]. However, functionality of
467 these Neocallimastigomycete proteins in an oxygen-independent pathway for synthesis
468 of quinolinate from L-aspartate [19, 20] had not been demonstrated until now.

469 Neocallimastigomycetes appear to have acquired *nadB* from a proteobacterium while a
470 eukaryotic donor was implicated in the acquisition of *nadA* [6]. Our results demonstrate

471 that expression of *nadB* and *nadA* homologs, either from the Neocallimastigomycete *P.*
472 *finnis* or from the plant *A. thaliana* [21], suffice to allow anaerobic synthesis of NAD⁺ of *S.*
473 *cerevisiae*. Due to the involvement of the Bna2 and Bna4 oxygenases in NAD⁺ synthesis by
474 *S. cerevisiae*, nicotinate is an essential growth factor for this yeast under anaerobic
475 conditions [14, 54, 55]. The present study represents the first demonstration of a
476 metabolic engineering strategy to eliminate oxygen requirements for NAD⁺ synthesis in
477 this yeast. A similar strategy was successfully applied to enable oxygen-independent
478 synthesis of pyridine nucleotides in the bacterium *Pseudomonas putida* [56].
479 Functional expression of heterologous NadA quinolinate synthases in *S. cerevisiae* was
480 observed despite the fact that these enzymes are 4Fe-4S iron-sulfur cluster proteins [57,
481 58], which are notoriously difficult to functionally express in the yeast cytosol [59-62].
482 However, earlier studies on functional expression of the 4Fe-4S activating protein of
483 bacterial pyruvate-formate lyase [63, 64] demonstrated that low-levels of expression can
484 occur without modification of the yeast machinery for cytosolic assembly of Fe-S clusters.
485 The inability of *AtNadB* and *AtNadA* to support NAD⁺ synthesis in aerobic cultures may be
486 due to oxygen-sensitivity of the 4Fe-4S cluster in the *AtNadA* quinolinate synthase domain
487 [65]. In contrast to *PfNadA*, *AtNadA* carries an N-terminal SufE domain which, in other
488 organisms, has been demonstrated to allow this oxygen sensitive enzyme to remain active
489 under aerobic conditions by reconstituting its Fe-S cluster [65].
490 Whereas an alternative to the kynurnine pathway for NAD⁺ synthesis was previously
491 inferred from genome sequence analysis, the pathway by which Neocallimastigomycetes
492 synthesize Coenzyme A had not previously been explored. Six pathways for synthesis of
493 the essential CoA precursor β -alanine are known: (1) decarboxylation of L-aspartate [66],
494 (2) transamination of malonate semialdehyde with L-glutamate as aminodonor [67] or L-
495 alanine [68], (3) by reduction of uracil followed by hydrolysis of the resulting

496 dihydrouracil [69], (4) oxidative cleavage of spermine to 3-aminopropanal followed by
497 oxidation of the aldehyde group [16], (5) 2,3-aminomutase of alanine [70], and (6)
498 addition of ammonia to acryloyl-CoA, followed by hydrolysis of the resulting CoA thioester
499 [70]. Of these pathways, the options (1), (2), (3), (5), and (6) can, in principle, occur in the
500 absence of oxygen. Yeasts and other filamentous fungi typically form β -alanine from
501 spermine (pathway 4), but in some species the use of pathway 3 was also reported [71].
502 While the aspartate decarboxylation route has not previously been demonstrated in wild-
503 type fungi, functional expression of bacterial and *T. castaneum* TcPanD was used in
504 metabolic engineering of *S. cerevisiae* to boost supply of β -alanine as a precursor for 3-
505 hydroxypropionate production [22, 50]. Phylogenetic analysis of putative members of the
506 pyridoxal-dependent L-aspartate decarboxylase family encoded by genomes of
507 Neocallimastigomycetes allowed for identification of *NcadcA* which complemented a
508 pantothenate-auxotrophic mutant of *S. cerevisiae*.

509 Amino acid sequence analysis of the characterised *NcAdcA* (A0A1Y1ZL74) yielded the
510 highest homology with sequences from chytrid fungi and *Clostridium* bacteria. This
511 observation is in agreement with previous research showing that HGT events played a
512 major role in shaping the genomes of Neocallimastigomycota [4, 6, 7], with Clostridiales
513 as important sequence donors [6]. Phylogenetic analysis of Adc sequences (Fig. 2) are
514 consistent with an earlier report on multiple evolutionary origins and variable
515 evolutionary rates of pyridoxal-5'-phosphate-dependent enzymes, including Adcs and
516 glutamate decarboxylases [72, 73]. A separate clade of Neocallimastigomycete sequences
517 show homology with characterised glutamate decarboxylases (e.g. Q04792 from *S.*
518 *cerevisiae* and K4H XK6 from *Lactobacillus brevis*; Fig 2. These results further support
519 acquisition of an Adc encoding DNA sequence by HGT rather than by neofunctionalization
520 of a glutamate decarboxylase gene.

521 Wild-type *S. cerevisiae* strains cannot grow in anaerobic environments unless
522 supplemented with pantothenate. Expression of either *NcadcA* or *TcPAND* in an *fms1Δ S.*
523 *cerevisiae* strain, which lacks the native oxygen-dependent pantothenate biosynthesis
524 pathway, enabled growth in pantothenate-free medium under aerobic and anaerobic
525 conditions. Although the different specific growth rates of *S. cerevisiae* strains expressing
526 *NcadcA* or *TcPAND* indicate that changing expression levels and/or origin of ADC
527 encoding genes may be required to achieve optimal growth, these results provide a proof-
528 of-principle for a simple metabolic engineering strategy to eliminate oxygen
529 requirements for pantothenate synthesis.

530 This work contributes to the understanding of how Neocallimastigomycetes adapted to
531 their anaerobic lifestyle by acquiring genes that enable oxygen-independent synthesis of
532 central metabolic cofactors. Experiments with engineered *S. cerevisiae* strains showed
533 that contribution of the heterologous genes to *in vivo* oxygen-independent cofactor
534 synthesis did not require additional mutations in the host genome. These results indicate
535 how acquisition of functional genes by HGT, even if their expression was initially
536 suboptimal, could have conferred an immediate advantage to ancestors of anaerobic fungi
537 living in cofactor-limited anoxic environments. A similar approach was recently applied
538 to study the physiological impact on *S. cerevisiae* of expressing a heterologous gene
539 encoding squalene-tetrahymanol cyclase, which in Neocallimastigomycetes produces the
540 sterol surrogate tetrahymanol [13]. Functional analysis by heterologous expression in *S.*
541 *cerevisiae* circumvents the current lack of tools for genetic modification of
542 Neocallimastigomycetes [2], and can complement biochemical studies [3-5] and genome
543 sequence analyses [6, 7].

544 Pantothenate and nicotinate, together with the other compounds belonging to the B-
545 group of water-soluble vitamins, are standard ingredients of chemically defined media for

546 aerobic and anaerobic cultivation of yeasts [48]. *S. cerevisiae* strains have been shown to
547 contain the genetic information required for *de novo* synthesis of these vitamins and, can
548 even be experimentally evolved for complete prototrophy for individual vitamins by
549 prolonged cultivation in single-vitamin depleted media [74, 75]. In large-scale processes,
550 addition of nutritional supplements increases costs, reduces shelf-life of media and
551 increases the risk of contamination during their storage [48]. Therefore, metabolic
552 engineering strategies for enabling oxygen-independent synthesis of NAD⁺ and
553 pantothenate are of particular interest for the development robust yeast strains with
554 minimal nutritional requirements that can be applied in anaerobic biofuels production
555 [48]. Further studies of the unique evolutionary adaptations of Neocallimastigomycetes
556 may well provide additional inspiration for engineering robust fungal cell factories that
557 operate under anaerobic conditions.

558 **References**

- 559 1. Gruninger RJ, Puniya AK, Callaghan TM, Edwards JE, Youssef N, Dagar SS, et al.
560 Anaerobic fungi (phylum Neocallimastigomycota): advances in understanding their
561 taxonomy, life cycle, ecology, role and biotechnological potential. *FEMS Microbiol Ecol.*
562 2014;**90**:1-17.
- 563 2. Wilken SE, Seppala S, Lankiewicz TS, Saxena M, Henske JK, Salamov AA, et al.
564 Genomic and proteomic biases inform metabolic engineering strategies for anaerobic
565 fungi. *Metab Eng Commun.* 2020;**10**:e00107.
- 566 3. Kemp P, Lander DJ, Orpin CG. The lipids of the rumen fungus *Piromonas communis*.
567 *J Gen Microbiol.* 1984;**130**:27-37.
- 568 4. Garcia-Vallve S, Romeu A, Palau J. Horizontal gene transfer of glycosyl hydrolases
569 of the rumen fungi. *Mol Biol Evol.* 2000;**17**:352-61.

- 570 5. Harhangi HR, Akhmanova AS, Emmens R, van der Drift C, de Laat WT, van Dijken
571 JP, et al. Xylose metabolism in the anaerobic fungus *Piromyces* sp. strain E2 follows the
572 bacterial pathway. *Arch Microbiol.* 2003;**180**:134-41.
- 573 6. Murphy CL, Youssef NH, Hanafy RA, Couger MB, Stajich JE, Wang Y, et al. Horizontal
574 gene transfer as an indispensable driver for evolution of Neocallimastigomycota into a
575 distinct gut-dwelling fungal lineage. *Appl Environ Microbiol.* 2019;**85**:e00988-19.
- 576 7. Youssef NH, Couger MB, Struchtemeyer CG, Liggenstoffer AS, Prade RA, Najjar FZ,
577 et al. The genome of the anaerobic fungus *Orpinomyces* sp. strain C1A reveals the unique
578 evolutionary history of a remarkable plant biomass degrader. *Appl Environ Microbiol.*
579 2013;**79**:4620-34.
- 580 8. Wang Y, Youssef NH, Couger MB, Hanafy RA, Elshahed MS, Stajich JE. Molecular
581 dating of the emergence of anaerobic rumen fungi and the impact of laterally acquired
582 genes. *mSystems.* 2019;**4**.
- 583 9. Weete JD, Abril M, Blackwell M. Phylogenetic distribution of fungal sterols. *Plos*
584 *One.* 2010;**5**:e10899.
- 585 10. Summons RE, Bradley AS, Jahnke LL, Waldbauer JR. Steroids, triterpenoids and
586 molecular oxygen. *Philos T R Soc B.* 2006;**361**:951-68.
- 587 11. Ourisson G, Rohmer M, Poralla K. Prokaryotic hopanoids and other polyterpenoid
588 sterol surrogates. *Annu Rev Microbiol.* 1987;**41**:301-33.
- 589 12. Takishita K, Chikaraishi Y, Leger MM, Kim E, Yabuki A, Ohkouchi N, et al. Lateral
590 transfer of tetrahymanol-synthesizing genes has allowed multiple diverse eukaryote
591 lineages to independently adapt to environments without oxygen. *Biol Direct.* 2012;**7**.
- 592 13. Wiersma SJ, Mooiman C, Giera M, Pronk JT. Expression of a squalene-tetrahymanol
593 cyclase enables sterol-independent growth of *Saccharomyces cerevisiae*. *Appl Environ*
594 *Microbiol.* 2020.

- 595 14. Panozzo C, Nawara M, Suski C, Kucharczyka R, Skoneczny M, Becam AM, et al.
596 Aerobic and anaerobic NAD⁺ metabolism in *Saccharomyces cerevisiae*. *FEBS Lett*.
597 2002;**517**:97-102.
- 598 15. Landry J, Sternglanz R. Yeast Fms1 is a FAD-utilizing polyamine oxidase. *Biochem*
599 *Bioph Res Co*. 2003;**303**:771-6.
- 600 16. White WH, Gunyuzlu PL, Toyn JH. *Saccharomyces cerevisiae* is capable of *de novo*
601 pantothenic acid biosynthesis involving a novel pathway of β -alanine production from
602 spermine. *J Biol Chem*. 2001;**276**:10794-800.
- 603 17. White WH, Skatrud PL, Xue ZX, Toyn JH. Specialization of function among aldehyde
604 dehydrogenases: The *ALD2* and *ALD3* genes are required for β -alanine biosynthesis in
605 *Saccharomyces cerevisiae*. *Genetics*. 2003;**163**:69-77.
- 606 18. Orpin CG, Greenwood Y. Nutritional and germination requirements of the rumen
607 chytridiomycete *Neocallimastix patriciarum*. *T Brit Mycol Soc*. 1986;**86**:103-9.
- 608 19. Hao JF, Petriacq P, de Bont L, Hodges M, Gakiere B. Characterization of L-aspartate
609 oxidase from *Arabidopsis thaliana*. *Plant Sci*. 2018;**271**:133-42.
- 610 20. Tedeschi G, Negri A, Mortarino M, Ceciliani F, Simonic T, Faotto L, et al. L-aspartate
611 oxidase from *Escherichia coli*. II. Interaction with C4 dicarboxylic acids and identification
612 of a novel L-aspartate:fumarate oxidoreductase activity. *Eur J Biochem*. 1996;**239**:427-33.
- 613 21. Katoh A, Uenohara K, Akita M, Hashimoto T. Early steps in the biosynthesis of NAD
614 in *Arabidopsis* start with aspartate and occur in the plastid. *Plant Physiol*. 2006;**141**:851-
615 7.
- 616 22. Arakane Y, Lomakin J, Beeman RW, Muthukrishnan S, Gehrke SH, Kanost MR, et al.
617 Molecular and functional analyses of amino acid decarboxylases involved in cuticle
618 tanning in *Tribolium castaneum*. *J Biol Chem*. 2009;**284**:16584-94.

- 619 23. Entian KD, Kotter P. 25 yeast genetic strain and plasmid collections. *Methods in*
620 *microbiology*. 2007;**36**:629-66.
- 621 24. Verduyn C, Postma E, Scheffers WA, Van Dijken JP. Effect of benzoic acid on
622 metabolic fluxes in yeasts: a continuous-culture study on the regulation of respiration and
623 alcoholic fermentation. *Yeast*. 1992;**8**:501-17.
- 624 25. Luttik MA, Kotter P, Salomons FA, van der Klei IJ, van Dijken JP, Pronk JT. The
625 *Saccharomyces cerevisiae* *ICL2* gene encodes a mitochondrial 2-methylisocitrate lyase
626 involved in propionyl-coenzyme A metabolism. *J Bacteriol*. 2000;**182**:7007-13.
- 627 26. Solis-Escalante D, Kuijpers NG, Bongaerts N, Bolat I, Bosman L, Pronk JT, et al.
628 amdSYM, a new dominant recyclable marker cassette for *Saccharomyces cerevisiae*. *FEMS*
629 *Yeast Res*. 2013;**13**:126-39.
- 630 27. Dekker WJC, Wiersma SJ, Bouwknecht J, Mooiman C, Pronk JT. Anaerobic growth of
631 *Saccharomyces cerevisiae* CEN.PK113-7D does not depend on synthesis or
632 supplementation of unsaturated fatty acids. *FEMS Yeast Res*. 2019;**19**:foz060.
- 633 28. Mans R, van Rossum HM, Wijsman M, Backx A, Kuijpers NG, van den Broek M, et al.
634 CRISPR/Cas9: a molecular Swiss army knife for simultaneous introduction of multiple
635 genetic modifications in *Saccharomyces cerevisiae*. *FEMS Yeast Res*. 2015;**15**:fov004.
- 636 29. Looke M, Kristjuhan K, Kristjuhan A. Extraction of genomic DNA from yeasts for
637 PCR-based applications. *Biotechniques*. 2011;**50**:325-.
- 638 30. Gietz RD, Woods RA. Transformation of yeast by lithium acetate/single-stranded
639 carrier DNA/polyethylene glycol method. *Method Enzymol*. 2002;**350**:87-96.
- 640 31. Inoue H, Nojima H, Okayama H. High efficiency transformation of *Escherichia coli*
641 with plasmids. *Gene*. 1990;**96**:23-8.

- 642 32. Gibson DG, Young L, Chuang RY, Venter JC, Hutchison CA, Smith HO. Enzymatic
643 assembly of DNA molecules up to several hundred kilobases. *Nat Methods*. 2009;**6**:343-
644 U41.
- 645 33. Mans R, Wijsman M, Daran-Lapujade P, Daran JM. A protocol for introduction of
646 multiple genetic modifications in *Saccharomyces cerevisiae* using CRISPR/Cas9. *FEMS*
647 *Yeast Res*. 2018;**18**.
- 648 34. Lee ME, DeLoache WC, Cervantes B, Dueber JE. A highly characterized yeast toolkit
649 for modular, multipart assembly. *Acs Synth Biol*. 2015;**4**:975-86.
- 650 35. DiCarlo JE, Norville JE, Mali P, Rios X, Aach J, Church GM. Genome engineering in
651 *Saccharomyces cerevisiae* using CRISPR-Cas systems. *Nucleic Acids Res*. 2013;**41**:4336-43.
- 652 36. Verhoeven MD, Lee M, Kamoen L, van den Broek M, Janssen DB, Daran JMG, et al.
653 Mutations in *PMR1* stimulate xylose isomerase activity and anaerobic growth on xylose of
654 engineered *Saccharomyces cerevisiae* by influencing manganese homeostasis. *Sci Rep-Uk*.
655 2017;**7**:46155.
- 656 37. Medina VG, Almering MJH, van Maris AJA, Pronk JT. Elimination of glycerol
657 production in anaerobic cultures of a *Saccharomyces cerevisiae* strain engineered to use
658 acetic acid as an electron acceptor. *Appl Environ Microb*. 2010;**76**:190-5.
- 659 38. Tomita H, Yokooji Y, Ishibashi T, Imanaka T, Atomi H. An archaeal glutamate
660 decarboxylase homolog functions as an aspartate decarboxylase and is involved in β -
661 alanine and coenzyme A biosynthesis. *J Bacteriol*. 2014;**196**:1222-30.
- 662 39. Camacho C, Coulouris G, Avagyan V, Ma N, Papadopoulos J, Bealer K, et al. BLAST+:
663 architecture and applications. *BMC Bioinformatics*. 2009;**10**:421.
- 664 40. Mistry J, Finn RD, Eddy SR, Bateman A, Punta M. Challenges in homology search:
665 HMMER3 and convergent evolution of coiled-coil regions. *Nucleic Acids Res*.
666 2013;**41**:e121.

- 667 41. Sievers F, Wilm A, Dineen D, Gibson TJ, Karplus K, Li W, et al. Fast, scalable
668 generation of high-quality protein multiple sequence alignments using Clustal Omega. *Mol*
669 *Syst Biol.* 2011;**7**:539.
- 670 42. Kozlov AM, Darriba D, Flouri T, Morel B, Stamatakis A. RAxML-NG: a fast, scalable
671 and user-friendly tool for maximum likelihood phylogenetic inference. *Bioinformatics.*
672 2019;**35**:4453-5.
- 673 43. Letunic I, Bork P. Interactive Tree Of Life (iTOL) v4: recent updates and new
674 developments. *Nucleic Acids Res.* 2019;**47**:W256-W9.
- 675 44. Li H, Durbin R. Fast and accurate short read alignment with Burrows-Wheeler
676 transform. *Bioinformatics.* 2009;**25**:1754-60.
- 677 45. Salazar AN, Gorter de Vries AR, van den Broek M, Wijsman M, de la Torre Cortes P,
678 Brickwedde A, et al. Nanopore sequencing enables near-complete *de novo* assembly of
679 *Saccharomyces cerevisiae* reference strain CEN.PK113-7D. *FEMS Yeast Res.* 2017;**17**.
- 680 46. Li H, Handsaker B, Wysoker A, Fennell T, Ruan J, Homer N, et al. The Sequence
681 Alignment/Map format and SAMtools. *Bioinformatics.* 2009;**25**:2078-9.
- 682 47. Walker BJ, Abeel T, Shea T, Priest M, Abouelliel A, Sakthikumar S, et al. Pilon: an
683 integrated tool for comprehensive microbial variant detection and genome assembly
684 improvement. *PLoS One.* 2014;**9**:e112963.
- 685 48. Perli T, Wronska AK, Ortiz-Merino RA, Pronk JT, Daran JM. Vitamin requirements
686 and biosynthesis in *Saccharomyces cerevisiae*. *Yeast.* 2020;**37**:283-304.
- 687 49. Vermeersch L, Perez-Samper G, Cerulus B, Jariani A, Gallone B, Voordeckers K, et
688 al. On the duration of the microbial lag phase. *Curr Genet.* 2019;**65**:721-7.
- 689 50. Borodina I, Kildegaard KR, Jensen NB, Blicher TH, Maury J, Sherstyk S, et al.
690 Establishing a synthetic pathway for high-level production of 3-hydroxypropionic acid in
691 *Saccharomyces cerevisiae* via β -alanine. *Metab Eng.* 2015;**27**:57-64.

- 692 51. Papapetridis I, van Dijk M, Dobbe APA, Metz B, Pronk JT, van Maris AJA. Improving
693 ethanol yield in acetate-reducing *Saccharomyces cerevisiae* by cofactor engineering of 6-
694 phosphogluconate dehydrogenase and deletion of *ALD6*. *Microb Cell Fact.* 2016;**15**:67.
- 695 52. Visser W, Scheffers WA, Batenburg-van der Vegte WH, van Dijken JP. Oxygen
696 requirements of yeasts. *Appl Environ Microbiol.* 1990;**56**:3785-92.
- 697 53. da Costa BLV, Basso TO, Raghavendran V, Gombert AK. Anaerobiosis revisited:
698 growth of *Saccharomyces cerevisiae* under extremely low oxygen availability. *Appl*
699 *Microbiol Biotechnol.* 2018;**102**:2101-16.
- 700 54. Ahmad F, Moat AG. Nicotinic acid biosynthesis in prototrophs and tryptophan
701 auxotrophs of *Saccharomyces cerevisiae*. *J Biol Chem.* 1966;**241**:775-80.
- 702 55. Suomalainen H, Nurminen T, Vihervaara K, Oura E. Effect of aeration on the
703 synthesis of nicotinic acid and nicotinamide adenine dinucleotide by baker's yeast. *J Inst*
704 *Brew.* 1965;**71**:227-31.
- 705 56. Kampers LFC, van Heck RGA, Donati S, Saccenti E, Volkers RJM, Schaap PJ, et al. In
706 silico-guided engineering of *Pseudomonas putida* towards growth under micro-oxic
707 conditions. *Microb Cell Fact.* 2019;**18**:179.
- 708 57. Rousset C, Fontecave M, Ollagnier de Choudens S. The [4Fe-4S] cluster of
709 quinolinate synthase from *Escherichia coli*: investigation of cluster ligands. *FEBS Lett.*
710 2008;**582**:2937-44.
- 711 58. Saunders AH, Griffiths AE, Lee KH, Cicchillo RM, Tu L, Stromberg JA, et al.
712 Characterization of quinolinate synthases from *Escherichia coli*, *Mycobacterium*
713 *tuberculosis*, and *Pyrococcus horikoshii* indicates that [4Fe-4S] clusters are common
714 cofactors throughout this class of enzymes. *Biochemistry.* 2008;**47**:10999-1012.

- 715 59. Zou R, Zhou K, Stephanopoulos G, Too HP. Combinatorial engineering of 1-deoxy-
716 D-xylulose 5-phosphate pathway using cross-lapping in vitro assembly (CLIVA) method.
717 *PLoS One*. 2013;**8**:e79557.
- 718 60. Carlsen S, Ajikumar PK, Formenti LR, Zhou K, Phon TH, Nielsen ML, et al.
719 Heterologous expression and characterization of bacterial 2-C-methyl-D-erythritol-4-
720 phosphate pathway in *Saccharomyces cerevisiae*. *Appl Microbiol Biotechnol*.
721 2013;**97**:5753-69.
- 722 61. Partow S, Siewers V, Daviet L, Schalk M, Nielsen J. Reconstruction and evaluation
723 of the synthetic bacterial MEP pathway in *Saccharomyces cerevisiae*. *PLoS One*.
724 2012;**7**:e52498.
- 725 62. Benisch F, Boles E. The bacterial Entner-Doudoroff pathway does not replace
726 glycolysis in *Saccharomyces cerevisiae* due to the lack of activity of iron-sulfur cluster
727 enzyme 6-phosphogluconate dehydratase. *J Biotechnol*. 2014;**171**:45-55.
- 728 63. Waks Z, Silver PA. Engineering a synthetic dual-organism system for hydrogen
729 production. *Appl Environ Microbiol*. 2009;**75**:1867-75.
- 730 64. Kozak BU, van Rossum HM, Benjamin KR, Wu L, Daran JM, Pronk JT, et al.
731 Replacement of the *Saccharomyces cerevisiae* acetyl-CoA synthetases by alternative
732 pathways for cytosolic acetyl-CoA synthesis. *Metab Eng*. 2014;**21**:46-59.
- 733 65. Murthy NM, Ollagnier-de-Choudens S, Sanakis Y, Abdel-Ghany SE, Rousset C, Ye H,
734 et al. Characterization of *Arabidopsis thaliana* SufE2 and SufE3: functions in chloroplast
735 iron-sulfur cluster assembly and NAD synthesis. *J Biol Chem*. 2007;**282**:18254-64.
- 736 66. Ramjee MK, Genschel U, Abell C, Smith AG. *Escherichia coli* L-aspartate- α -
737 decarboxylase: preprotein processing and observation of reaction intermediates by
738 electrospray mass spectrometry. *Biochem J*. 1997;**323 (Pt 3)**:661-9.

- 739 67. Tamaki N, Aoyama H, Kubo K, Ikeda T, Hama T. Purification and properties of β -
740 alanine aminotransferase from rabbit liver. *J Biochem.* 1982;**92**:1009-17.
- 741 68. Hayaishi O, Nishizuka Y, Tatibana M, Takeshita M, Kuno S. Enzymatic studies on
742 the metabolism of β -alanine. *J Biol Chem.* 1961;**236**:781-90.
- 743 69. Schnackerz KD, Dobritzsch D. Amidohydrolases of the reductive pyrimidine
744 catabolic pathway purification, characterization, structure, reaction mechanisms and
745 enzyme deficiency. *Biochim Biophys Acta.* 2008;**1784**:431-44.
- 746 70. Dalluge JJ, Liao H, Gokarn R, Jessen H. Discovery of enzymatic activity using stable
747 isotope metabolite labeling and liquid chromatography-mass spectrometry. *Anal Chem.*
748 2005;**77**:6737-40.
- 749 71. Gojkovic Z, Sandrini MP, Piskur J. Eukaryotic β -alanine synthases are functionally
750 related but have a high degree of structural diversity. *Genetics.* 2001;**158**:999-1011.
- 751 72. Sandmeier E, Hale TI, Christen P. Multiple evolutionary origin of pyridoxal-5'-
752 phosphate-dependent amino acid decarboxylases. *Eur J Biochem.* 1994;**221**:997-1002.
- 753 73. Salzmann D, Christen P, Mehta PK, Sandmeier E. Rates of evolution of pyridoxal-5'-
754 phosphate-dependent enzymes. *Biochem Biophys Res Commun.* 2000;**270**:576-80.
- 755 74. Perli T, Moonen DPI, van den Broek M, Pronk JT, Daran JM. Adaptive laboratory
756 evolution and reverse engineering of single-vitamin prototrophies in *Saccharomyces*
757 *cerevisiae*. *Appl Environ Microbiol.* 2020;**86**:e00388-20.
- 758 75. Bracher JM, de Hulster E, Koster CC, van den Broek M, Daran JG, van Maris AJA, et
759 al. Laboratory evolution of a biotin-requiring *Saccharomyces cerevisiae* strain for full
760 biotin prototrophy and identification of causal mutations. *Appl Environ Microbiol.*
761 2017;**83**.
- 762 76. Papapetridis I, Goudriaan M, Vazquez Vitali M, de Keijzer NA, van den Broek M, van
763 Maris AJA, et al. Optimizing anaerobic growth rate and fermentation kinetics in

764 *Saccharomyces cerevisiae* strains expressing Calvin-cycle enzymes for improved ethanol
765 yield. *Biotechnol Biofuels*. 2018;**11**:17.

766 77. Wronska AK, Haak MP, Geraats E, Slot EB, van den Broek M, Pronk JT, et al.
767 Exploiting the diversity of Saccharomycotina yeasts to engineer biotin-independent
768 growth of *Saccharomyces cerevisiae*. *Appl Environ Microbiol*. 2020;**86**:e00270-20.

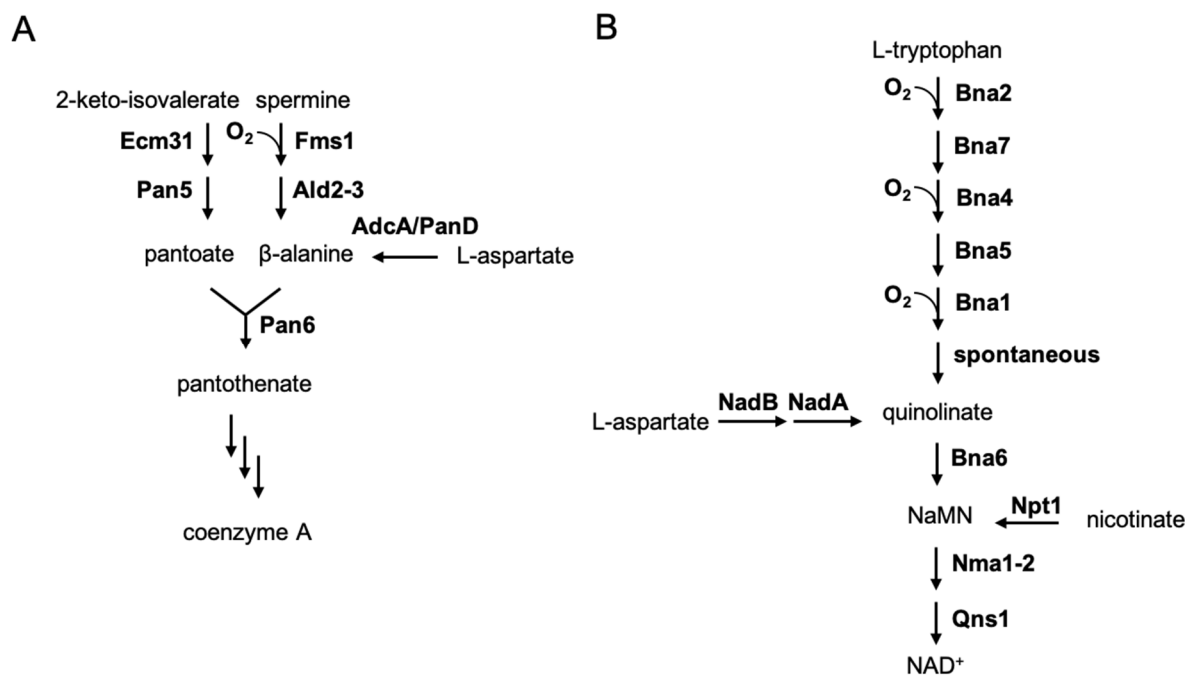
769 ***Acknowledgments***

770 We thank Dr. Irina Borodina for providing us the codon-optimized *TcPAND* gene and
771 Sabina Shrestha for constructing strain IMK877. TP and J-MD were supported by the
772 European Union's Horizon 2020 research and innovation programme under the Marie
773 Skłodowska-Curie action PACMEN (grant agreement No 722287). AMV, WJCD, JB, SJW,
774 RAO-M, CM and JTP were funded by an Advanced Grant of the European Research
775 Council to JTP (grant # 694633). Authors declare that they have no conflict of interests.

776 ***Author contributions***

777 All authors contributed to the experimental design. TP, AMV, JMD and JTP wrote a first
778 version of the manuscript. All authors critically read this version, provided input and
779 approved the final version. RAO-M, AMV, and TP performed the phylogenetic analysis. TP
780 constructed the *S. cerevisiae* strains and performed the aerobic characterization. AMV,
781 WJCD and TP performed the anaerobic chamber experiments. JB, CM, TP, AMV, and SJW
782 performed and analysed the bioreactor experiments.

783 **Figure legends**



784

785 **Fig. 1: CoA and NAD⁺ biosynthetic pathways in *S. cerevisiae* and oxygen-independent**

786 **alternatives.** CoA synthesis includes the condensation of pantoate and β-alanine. In *S.*

787 *cerevisiae* β-alanine is formed from spermine in two steps using the oxygen-dependent

788 poly-amine oxidase Fms1 (A). Other organisms, including archaea, bacteria, and insects,

789 can by-pass this oxygen requirement by synthesizing β-alanine from aspartate using L-

790 aspartate decarboxylase (AdcA/PanD). NAD⁺ is synthesized via the kynurenine pathway

791 in 9 reactions starting from tryptophan, 3 of which require oxygen (B). Other organisms

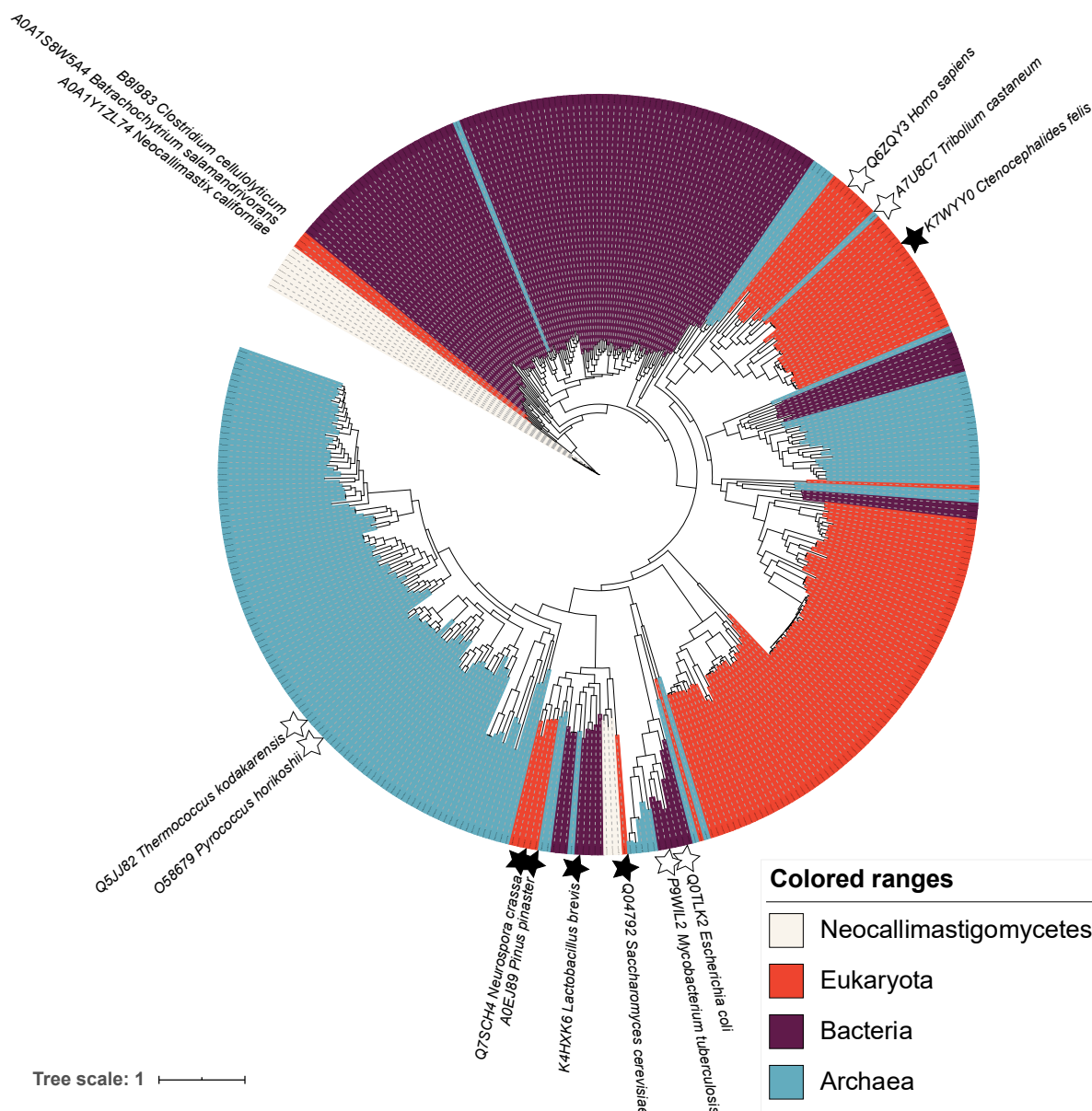
792 that include plants and bacteria are able to bypass this oxygen requirement by

793 synthesizing quinolinate from aspartate using L-aspartate oxidase and quinolinate

794 synthase (NadB and NadA, respectively)

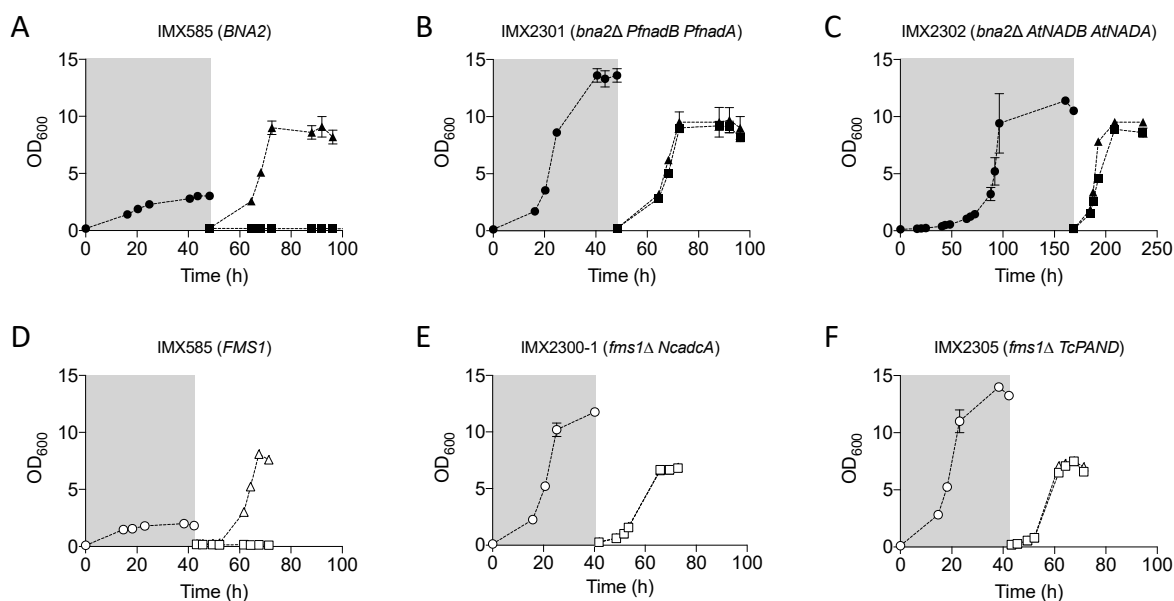
795

796



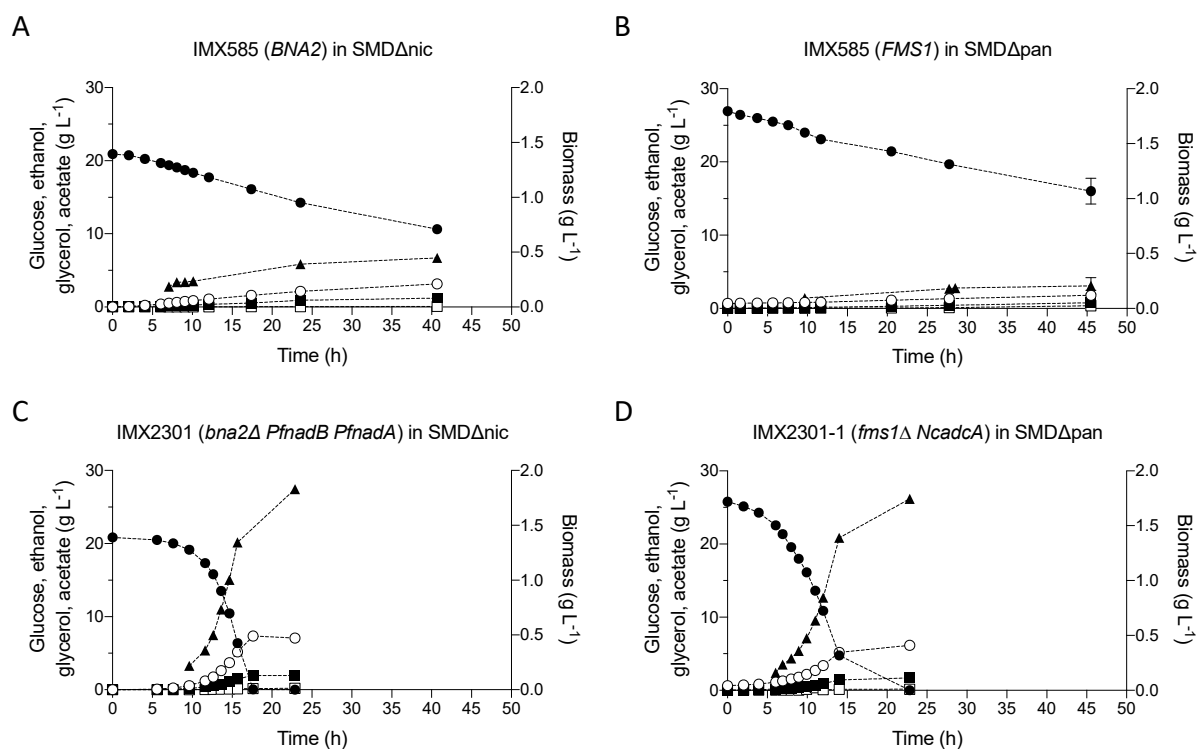
797

798 **Fig. 2: Maximum likelihood phylogenetic tree of aspartate decarboxylase and**
 799 **glutamate decarboxylase sequences.** Sequences of proteins with demonstrated
 800 enzyme activity are marked with white stars (L-aspartate decarboxylases) or black stars
 801 (glutamate decarboxylases). A version of this tree with all sequence identifiers, branch
 802 support, distances and bootstrap values, is provided in the Supplementary File 2. An
 803 interactive visualisation can be accessed in <https://itol.embl.de/shared/rortizmerino>



804

805 **Fig. 3: Anaerobic growth of *S. cerevisiae* strains dependent or independent on**
806 **supplementation of nicotinic acid (NA) or pantothenic acid (PA) in SMD medium**
807 **containing Tween 80 and ergosterol.** Strains IMX585 (A), IMX2301 (*bna2Δ PfnadB*
808 *PfnadA*) (B), and IMX2302 (*bna2Δ AtNADB AtNADA*) (C) transferred to medium with 2 %
809 glucose with (▲) or without (■) nicotinate after a carry-over phase in SMDΔnic containing
810 4 % glucose (● in grey box). Strains IMX585 (D), IMX2300-1 (*fms1Δ NcadcA*) (E), and
811 IMX2305 (*fms1Δ TcPAND*)(F) transferred to medium with (△) or without (□)
812 pantothenate after a carry-over phase in SMDΔpan containing 4 % glucose (○ in grey box).
813 Anaerobic condition in the chamber were maintained using a palladium catalyst and a 5
814 % hydrogen concentration. Error bars represent the mean deviation of independent
815 cultures (n=2)



816

817 **Fig. 4: Anaerobic batch cultivation of IMX585 in SMDΔnic (A) and SMDΔpan (B),**

818 **IMX2301 in SMDΔnic (C) and IMX2300-1 in SMDΔpan (D).** All strains were pre-

819 grown in the corresponding medium lacking one vitamin prior to inoculation in the

820 bioreactor to avoid carry-over effects. Values for glucose (●), ethanol (○), glycerol (■),

821 acetate (□) and biomass (▲) are shown over time. Error bars represent the mean

822 deviation of independent cultures (n=2)

823

824 **Tables**825 **Table 1: *S. cerevisiae* strains used in this study**

Name	Relevant genotype	Parental strain	Reference
CEN.PK113-7D	MATa <i>URA3</i>	-	[23]
CEN.PK113-5D	MATa <i>ura3-52</i>	-	[23]
IMX585	MATa <i>can1Δ::Spycas9-natNT2 URA3</i>	CEN.PK113-7D	[28]
IMX581	MATa <i>ura3-52 can1Δ::Spycas9-natNT2</i>	CEN.PK113-5D	[28]
IMX2292	MATa <i>can1Δ::Spycas9-natNT2 URA3 fms1Δ</i>	IMX585	[74]
IMK877	MATa <i>can1Δ::Spycas9-natNT2 URA3 bna2Δ</i>	IMX585	This study
IMX2301	MATa <i>can1Δ::Spycas9-natNT2 URA3 bna2Δ sga1::pTDH3-PfnadA-tENO1 pCCW12-PfnadB-tENO2</i>	IMK877	This study
IMX2302	MATa <i>can1Δ::Spycas9-natNT2 URA3 bna2Δ sga1::pTDH3-AtNADA-tENO1 pCCW12-AtNADB-tENO2</i>	IMK877	This study
IMX2293	MATa <i>ura3-52 can1Δ::Spycas9-natNT2 fms1Δ</i>	IMX581	This study
IMX2300	MATa <i>ura3-52::pTDH3-NcadC-tENO2 URA3 can1Δ::Spycas9-natNT2 fms1Δ</i>	IMX2293	This study
IMX2300-1	MATa <i>ura3-52::pTDH3-NcadC-tENO2 URA3 can1Δ::Spycas9-natNT2 fms1Δ</i> Colony isolate 1	IMX2300	This study
IMX2305	MATa <i>ura3-52::pRPL12b-TcPAND-tTDH1 URA3 can1Δ::Spycas9-natNT2 fms1Δ</i>	IMX2293	This study

826 *Spy*: *Streptococcus pyogenes*; *Pf*: *Piromyces finnis*; *Nc*: *Neocallimastix californiae*; *At*: *Arabidopsis thaliana*; *Tc*: *Tribolium castaneum*.

827 **Table 2: plasmids used in this study**

Name	Characteristics	Reference
pROS10	2 μ m <i>bla</i> ori <i>URA3</i> gRNA- <i>CAN1.Y</i> gRNA- <i>ADE2.Y</i>	[28]
pROS11	2 μ m <i>bla</i> ori amdSYM gRNA- <i>CAN1.Y</i> gRNA- <i>ADE2.Y</i>	[28]
pROS13	2 μ m <i>bla</i> ori kanMX gRNA- <i>CAN1.Y</i> gRNA- <i>ADE2.Y</i>	[28]
pUDR119	2 μ m <i>bla</i> ori amdSYM gRNA- <i>SGA1</i> gRNA- <i>SGA1</i>	[76]
pYTK009	p <i>TDH3 cat</i> ColE1	[34]
pYTK010	p <i>CCW12 cat</i> ColE1	[34]
pYTK017	p <i>RPL18B cat</i> ColE1	[34]
pYTK051	t <i>ENO1 cat</i> ColE1	[34]
pYTK055	t <i>ENO2 cat</i> ColE1	[34]
pYTK056	t <i>TDH1 cat</i> ColE1	[34]
pYTK096	ConLS' <i>gfp</i> ConRE' <i>URA3 nptII</i> ColE1 5' <i>URA3</i>	[34]
pGGKd017	ConLS' <i>gfp</i> ConRE' <i>URA3</i> 2 μ m <i>bla</i> ColE1	[77]
pCfB-361	2 μ m <i>bla</i> ori pTEF1- <i>TcPAND*</i> - <i>tCYC1 HIS3</i>	[50]
pUDR652	<i>bla</i> 2 μ m amdSYM gRNA- <i>FMS1</i> gRNA- <i>FMS1</i>	[74]
pUD652	<i>bla PfnadA*</i>	GeneArt, this study
pUD653	<i>bla PfnadB*</i>	GeneArt, this study
pUD1095	<i>bla NcadcA*</i>	GeneArt, this study
pUD1096	<i>bla AtNADA*</i>	GeneArt, this study
pUD1097	<i>nptII AtNADB*</i>	GeneArt, this study

pUDR315	<i>bla</i> 2 μ m <i>amdSYM</i> gRNA- <i>BNA2</i> gRNA- <i>BNA2</i>	This study
pUDI168	p <i>RPL18B</i> - <i>TcPAND</i> *-t <i>TDH1</i> <i>URA3 ntpII</i> ColE1 5' <i>URA3</i>	This study
pUDI242	p <i>TDH3</i> - <i>NcadcA</i> *-t <i>ENO2</i> <i>URA3 ntpII</i> ColE1 5' <i>URA3</i>	This study
pUDI243	p <i>TDH3</i> - <i>PfNADA</i> *-t <i>ENO1</i> <i>URA3 ntpII</i> ColE1 5' <i>URA3</i>	This study
pUDI244	p <i>CCW12</i> - <i>PfnadB</i> *-t <i>ENO2</i> <i>URA3 ntpII</i> ColE1 5' <i>URA3</i>	This study
pUDI245	p <i>TDH3</i> - <i>AtNADA</i> *-t <i>ENO1</i> <i>URA3 ntpII</i> ColE1 5' <i>URA3</i>	This study
pUDE931	p <i>CCW12</i> - <i>AtNADB</i> *-t <i>ENO2</i> <i>URA3</i> 2 μ m <i>bla</i> ColE1	This study

828 *Spy*: *Streptococcus pyogenes*; *Pf*: *Piromyces finnis*; *Nc*: *Neocallimastix californiae*; *At*: *Arabidopsis thaliana*; *Tc*: *Tribolium castaneum*.

829 *Codon-optimized for expression in *S. cerevisiae*.

830

831

832

833

834

835

836

837

838

839

840 **Table 3: Aerobic characterization of engineered strains.** Specific growth rates of *S. cerevisiae* strains grown in SMD, SMD Δ nic and
 841 SMD Δ pan media. The values are average and mean deviation of data from at least two independent cultures of each strain

Strain	SMD	SMD Δ nic	SMD Δ pan
IMX585 (<i>FMS1 BNA2</i>)	0.40 \pm 0.01	0.40 \pm 0.02	0.11 \pm 0.01
IMX2292(<i>fms1</i> Δ)	0.39 \pm 0.01		< 0.01
IMX2305 (<i>fms1</i> Δ <i>TcPAND</i>)	0.39 \pm 0.01		0.39 \pm 0.01
IMX2300-1 (<i>fms1</i> Δ <i>NcadcA</i>)	0.34 \pm 0.01		0.34 \pm 0.01
IMK877 (<i>bna2</i> Δ)	0.40 \pm 0.01	< 0.01	
IMX2301 (<i>bna2</i> Δ <i>PfnadB PfnadA</i>)	0.37 \pm 0.01	0.14 \pm 0.01	
IMX2302 (<i>bna2</i> Δ <i>AtNADB AtNADA</i>)	0.40 \pm 0.01	< 0.01	

842

843

844

845 **Table 4: Maximum specific growth rate (μ_{\max}) and yields of glycerol, biomass and ethanol on glucose in anaerobic bioreactor**
 846 **batch cultures of *S. cerevisiae* strains IMX585, IMX2301 and IMX2300-1.** Cultures were grown on SMD, SMD Δ nic, or SMD Δ pan,
 847 respectively, with 20 g L⁻¹ glucose as carbon source (pH = 5). Growth rates and yields were calculated from the exponential growth
 848 phase. The ethanol yield was corrected for evaporation. Values represent average and mean deviation of data from independent cultures
 849 (n = 2). Carbon recovery in all fermentations was between 95 and 100%

Strain	IMX585*	IMX2301	IMX2300-1
	(<i>FMS1 BNA2</i>)	(<i>bnA2Δ PfnadB PfnadA</i>)	(<i>fms1Δ NcadcA</i>)
Medium	SMD	SMD Δ nic	SMD Δ pan
μ_{\max} (h ⁻¹)	0.32 ± 0.00	0.31 ± 0.01	0.25 ± 0.00
Y glycerol/glucose (g g ⁻¹)	0.105 ± 0.000	0.103 ± 0.003	0.104 ± 0.000
Y biomass/glucose (g _x g ⁻¹)	0.094 ± 0.004	0.090 ± 0.002	0.081 ± 0.001
Y EtOH/glucose (g g ⁻¹)	0.372 ± 0.001	0.372 ± 0.002	0.364 ± 0.003

* data from [51]

850

851

852